CROATICA CHEMICA ACTA
CCACAA **76** (3) 207–215 (2003)

ISSN-0011-1643
CCA-2873
Original Scientific Paper

Ferromanganese Coated Structures from the Jabuka Pit (Central Adriatic): Mineralogical, Geochemical and Genetic Considerations

Tadej Dolenec

Department of Geology, Faculty of Natural Sciences and Engineering, University of Ljubljana, Aškerčeva 12, 1000 Ljubljana, Slovenia and Jožef Stefan Institute, Jamova 39, 1000 Ljubljana, Slovenia (E-mail: tadej.dolenec@ntfgeo.uni-lj.si)

RECEIVED FEBRUARY 6, 2002; REVISED FEBRUARY 13, 2003; ACCEPTED FEBRUARY 21, 2003

Key words
ferromanganese coating structures
10 Å manganates
SEM and EDS
geochemistry
Jabuka Pit
Central Adriatic

One of the most interesting features of the Jabuka Pit, a depression up to 275 m deep in the Central Adriatic is the presence of ferromanganese crusts and coatings found on various mollusks shells, shell fragments and other biogenic detritus exposed to seawater. They are composed mostly of Fe-poor and Mg-rich 10 Å manganates. 10 Å manganates also form collomorph-banded and botryoidal aggregates, as well as 1.5 mm high stalactitic structures composed of up to 5 μm long plate-like crystals. Their hydrogenous precipitation at the sediment-water interface in oxygenated conditions is hypothesised.

INTRODUCTION

The Jabuka Pit represents a shallow, up to 275 m deep depression in the Central Adriatic, named after a small volcanic island which is situated about twenty kilometres E of the deepest part of the depression. According to Faganeli *et al*.,[1] the sediments of the Jabuka Pit are composed of pelites consisting of silty clay with 25–40 % of carbonates mostly of pelagic organisms.[1] Twenty-four kilometres WNW from Jabuka Island there is a submarine ridge, which most probably represents a sunken volcanic island of the same gabbroic composition as the islands of Jabuka and Svetac.[2] The age of the volcanic rocks from this area most probably correspond to Subboreal and Younger Dryas.[3]

The most significant feature of the Jabuka Pit is the remarkable enrichment of recent sediments from this area in Mn. Surficial sediments from the Jabuka Pit exhibit Mn concentrations mostly in the range from 1140 to 3760 ppm.[4] Even higher values of up to 4250 ppm for the sediments of the same area were reported by Kosta *et al*.[5] The suspected main source of Mn concentrations in the surficial sediments of the Jabuka Pit is most probably submarine weathering of gabbroic rocks of the islands of Jabuka and Svetac, as well as pyroclastic materials from these areas. Contamination from the manganese processing plant located in Šibenik Bay may have also contributed to higher concentrations of Mn in the Jabuka Pit.[4] Up to now, there is no indication of any recent hydrothermal or geothermal influence on the supply of Mn or other metals to the sediments.

Another notable feature of the Jabuka Pit is the presence of ferromanganese crusts and coatings on various mollusk shells, shell fragments and other biogenic detritus exposed to seawater.[6] A preliminary study revealed that the coated structures comprise a complex assemblage of materials, including 10 Å manganates, X-ray amorphous iron oxyhydroxides, as well as several detrital and authigenic minerals and hard parts of marine organisms.[6] Mollusk shells and other biogenic detritus appear to be essential for the nucleation and intimate intergrowth of

hydrated Mn and Fe oxides, as already observed by Burns and Burns.[7]

The purpose of this paper is to determine the main mineralogical and geochemical characteristics of ferromanganese coated structures from the Jabuka Pit and to discuss the possible mechanism of their deposition on mollusk shells and on other biogenic detritus.

EXPERIMENTAL

The deep water mollusk shells and shell fragments with ferromanganese coatings and crusts selected for this study were collected during summer in the years 1997–1999 by dredging the floor with fisherman's nets in the central part of the Jabuka Pit, which represents the deepest (up to 275 m deep) part of the Central Adriatic (Figure 1). The sampling was performed as a part of a larger study in the frame work of the Slovenian-Croatian Bilateral Project (Biogeochemical processes, elemental and isotopic composition of the Adriatic Sea). During the collection of different biogenic carbonates from the Jabuka Pit for isotopic analyses, the mollusk shells covered with ferromanganese coatings were separated from biogenic carbonate skeletons without any visible coverings for further mineralogical and geochemical investigations. For this study ferromanganese coatings from 20 mollusk shells were chosen to create two composite samples (JP-103 and JP-104). Each composite sample consisted of 10 mollusk shells covered with earthy black ferromanganese crusts and stalactitic structures. In the laboratory the coatings were removed from the mollusk shells by a plastic knife and dried at ambient temperature and then homogenized by grinding in an agate mortar for geochemical and X-ray diffraction analyses. For characterization of the microstructure and composition of the coated structures, a sample of stalactitic aggregate grown on a mollusk shell and another sample from a mollusk shell covered with an about 30 μm thick ferromanganese crust were studied at the Jožef Stefan Institute with a JEOL JSM 5800 SEM instrument with Link ISIS 300 EDS. Quantitative analyses were performed using SEM Quand software and a virtual standard package library (VPS). Measured peak intensities in the spectra were corrected and quantified using a ZAF matrix correction program. For oxygen, semi-quantitative estimation is possible only by comparison between the peak areas of the oxygen peaks in different spectra without exact quantification. The relative random errors of EDS (Energy Dispersive Spectroscopy) were less than 6 % for the trace metals Ni, Co and Ba and better than 3 % for major and selected minor oxides.

The mineralogy was determined at the Department of Geology, Ljubljana, by X-ray powder diffractometry using a Philips PW 3710 diffractometer and Cu-Kα radiation. The two composite powdered samples (JP-103, JP-104) of ferromanganese crusts and stalactitic structures were scanned at a rate of 2° per minute, over the range of 2–70° (2Θ). The results were stored on a PC computer and analysed with PC-APD diffraction software. The diffraction patterns were identified using the data from the Powder Diffraction File (1977) JCPDS system (todorokite – JCPDF card numbers: 38-475, 13-164, 18-1411; birnessite – JCPDF card numbers: 43-1456, 23-1046 and 23-1239; buserite, a hydrous manga-

Figure 1. Map of the Adriatic Sea, showing the position of the Jabuka Pit and the location of the sampling area (■).

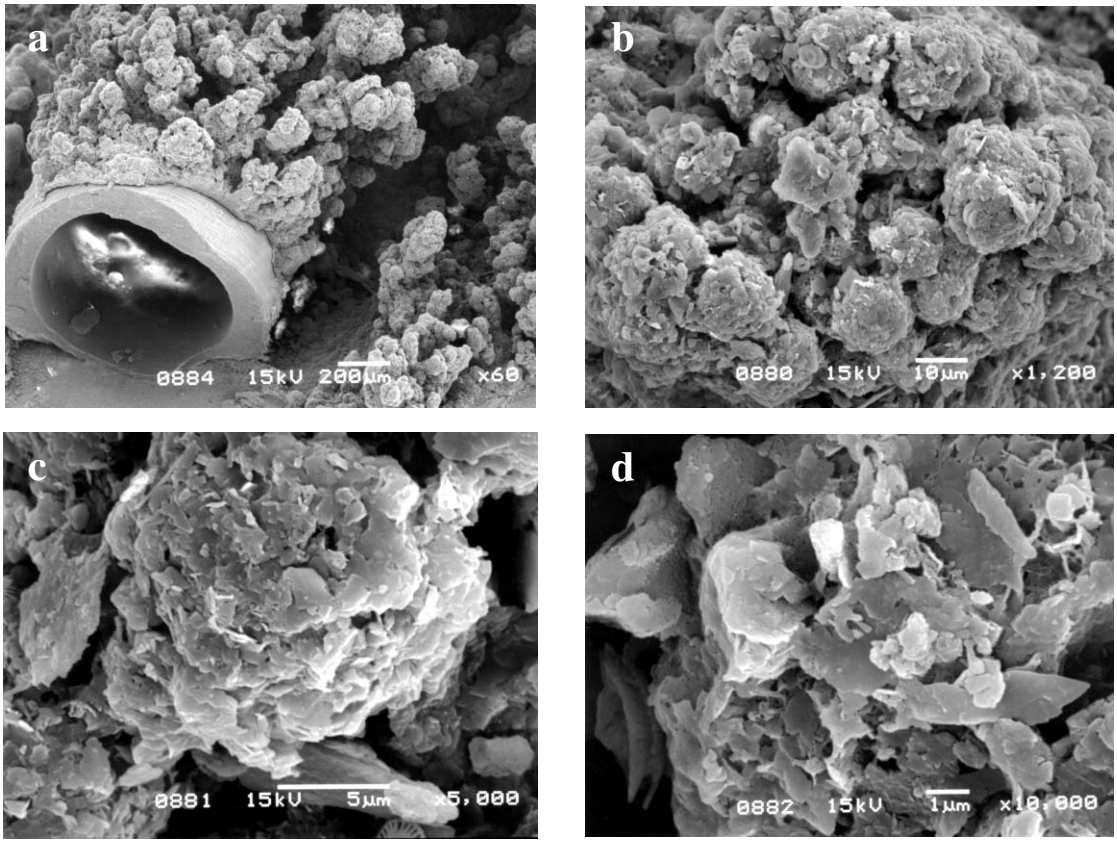

Figure 2. SEM photos of stalactitic ferromanganese aggregates on a *Serpula sp.* fragment at four different magnifications.

nate from the 10 Å todorokite group with 10 Å spacing, but with a layered rather than a tunnel structure – JCPDF card number 32-1128, vernadite – JCPDF card number 15-604) and data for synthetic todorokite from Bilinski *et al.*[8]

Samples JP-103 and JP-104 were also analysed by inductively coupled plasma-mass spectrometry (ICP/MS) for REE (La, Ce, Pr, Nd, Sm, Eu, Gd, Tb, Dy, Ho, Er, Yb, Lu), Rb, Nb, In, Mo, Sn, Cs, Ta, Hf, Tl, Sb, W, Pb, Bi, Th and U. Major (Si, Al, Fe, Mg, Ca, Na, K), minor (Mn, P, Ti) and selected trace elements (Ba, Sr, Y, Zr, Be, V) were measured after fusion with a mixture of lithium metaborate/lithium tetraborate and dissolution in nitric acid by ICP with a thermo Jarrell-Ash Enviro II ICP, while after total digestion by four acids (nitric, hydrochloric, perchloric and hydrofluoric) Cu, Zn, Ag, Ni, Co, Cd, Sc, As, An, Cr, Se and Hg were also determined by inductively coupled plasma (ICP) spectrometry. Calibration was achieved using a combination of CANMET and USGS reference materials. Concentrations of Se, Hg, Cd, Sn, Ag and In were generally lower than the detection limits of the selected ICP/MS and/or ICP methods (5, 1, 0.5, 0.5, 0.4 and 0.1 ppm, respectively). Elemental analyses were carried out at Activation Laboratories, Ontario, Canada. Analytical precision and accuracy were better than ±3 % for major elements, ±5 % for REE, but between 5 and 8 % for minor and the remaining trace elements. This was indicated by the results of duplicate measurements on one sample and the USGS MAG-1 (marine mud) and NOD-A-1 (Mn nodule) standards.

RESULTS

Shape, Occurrence, Size

Examination under an optical microscope showed that the ferromanganese crusts and coatings analysed during this study were generally earthy black. Their thickness varied from less than 5 to 500 µm. Mn and Fe hydrated oxides also formed collomorph-banded and rare botryoidal aggregates, which were a few tenths of a millimetre or less in diameter. Less commonly they occurred as 1.5 mm long black stalactitic structures with an earthy lustre growing on the surfaces of previously deposited crusts.

Scanning electron microscope examination showed various surface structures on the scale of a few micrometres *e.g.* aggregates of botryoidal clusters, spherulites, plates, and disks, as well as up to 5 µm long plate-like grains (Figure 2). At the highest magnification (10 000 x) one could see an isolated cluster mostly composed of disks and rare elongated acicular grains (Figure 2d). Biogenic debris, represented by coccoliths cemented by the manganese phase, was also common.

Backscattered electron examination of polished sections of stalactitic aggregates (Figure 3) revealed a laminated, more or less concentric banded pattern. Fragments of biogenic material and detrital minerals inside stalactitic aggregates were also observed.

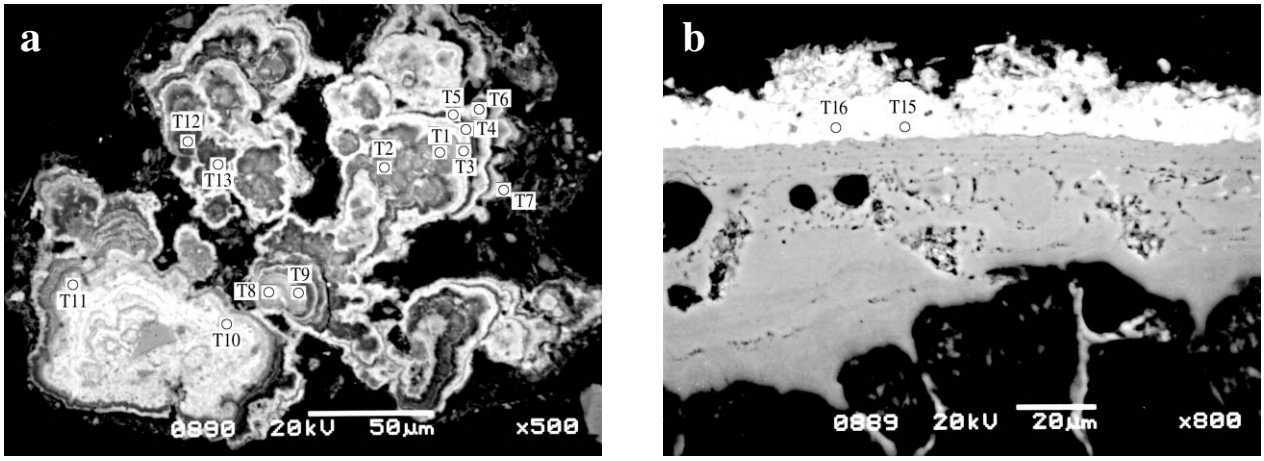

Figure 3. Backscattered electron micrograph of a polished section showing a vertical cross-section of the stalactitic ferromanganese aggregate (a) and the ferromanganese crust (b) growing on a mollusk shell. Points T1 to T16 refer to the EDS point count analysis presented in Table II.

Mineralogy

In the suite of ferromanganese crusts and coatings (samples JP-103 and JP-104), the main mineral phase was characterised by two relatively strong diagnostic peaks at 9.62 Å and 4.85 Å (sample JP-103) and at 9.64 and 4.84 Å (sample JP-104). The first and second order basal X-ray diffraction near 10 Å and 5 Å correspond to the reflection pattern of 10 Å manganates.[9] Complete data for the investigated samples are given in Table I, where X-ray diffraction data on the investigated samples are also compared with published data. The reference data are for a 10 Å manganate – todorokite from South Africa, $NaMn_6O_{12} \cdot 3H_2O$ (JCPDF card number 38-475), todorokite from the Todoroki mine, Japan, $(Mn^{II},Mg,Ca,Ba,K,Na)_2Mn^{IV}_5O_{12} \cdot 3H_2O$ (JCPDF card number 13-164), todorokite from the Charco Redondo deposit, Cuba, $(Mn,Ca,Ba,Na,K,Mg,Fe,Al)_3O_{7-y} \cdot (2-x)H_2O$, ($x$ and y = 0 to 1), (JCPDF card number 18-1411), synthetic todorokite prepared by Bilinski *et al.*,[8] 7 Å manganate birnessite, $Na_{0.55}Mn_2O_4 \cdot 1.5H_2O$ (JCPDF card number 43-1456) and $Na_4Mn_{14}O_{27} \cdot 9H_2O$ (JCPDF card number 23-1046), buserite, $Na_4Mn_{14}O_{27} \cdot 21H_2O$, a hydrous manganate that has a structure and composition analogous to synthetic 10 Å phyllomanganate (JCPDF card number 32-1128) as well as vernadite, $Mn(OH)_4$ (JCPDF card number 15-604). The observed peak intensities and their broadness may be a function of crystallinity as well as the abundance of 10 Å manganates in the composite samples. Other authigenic and/or detrital minerals including calcite (JCPDF card number 05-0586), dolomite (JCPDF card number 36-0426), aragonite (JCPDF card number 05-0543), mixed layer clays (illite/montmorilonite – JCPDF card number 35-0652), clinochlore (JCPDF card number 19-0749), muscovite-2M1 (JCPDF card number 06-0263), quartz (JCPDF card number 33-1161), feldspars (Albite – JCPDF card number 41-1480) and halite (JCPDF card number 05-0628) were also detected in minor to trace amounts.

Chemical Composition

A sample of a stalactitic aggregate and of a crust were analysed by EDS (Table II). Quantitative analysis carried out with the SEM-EDS system revealed the following elemental mass fractions (Table II): 43.2 to 60.4 % Mn, 0–3.6 % Fe, 4.3–7.4 % Mg, 1.2–5.7 % Ca, 1.2–5.0 % Al, 0.7–5.7 % Si, 0.1–1.4 % K, 0–2.4 % Na, 0–0.9 % Ba, 0.4–1.6 % Cl, 0–0.7 % Ni and 0–0.4 % Co. The Mn/Fe mass ratio was extremely variable with a minimum of 12.6. Some bright layers of stalactitic structures observed in backscattered electron photographs were somewhat richer in Mn and poorer in Fe content than darker ones, but this was not a rule. As no Fe phase was detected in the XRD scans of the coated structures, the bulk of the Fe must be present in some amorphous compound. A comparison between the peak areas of oxygen in the EDS spectra showed that the darker layers exhibited a lower oxygen peak than the lighter ones (Figure 4).

ICP and ICP/MS analyses of the two composite coated structure samples (JP-103 and JP-104), which also have minor amounts of detrital minerals embedded in them (Table III) showed that several trace elements such as Ba, Sr, Ni, Co, As, Pb, Cu and V were considerably enriched as compared to the surficial sediment (sample V-13) from the same locality, whereas Zn was present in only slightly higher concentrations. The REE fractions (ΣREE = 65 and 63 ppm) were lower relative to those of the surficial sediment ((ΣREE = 119 ppm). The PAAS (Post-Achaean average Australian shale[10]) normalized REE patterns (Figure 5) are roughly characterized by a relatively flat REE distribution and pronounced positive Ce and Eu anomalies with Ce/Ce* values of 1.33 and 1.45 and Eu/Eu* values of 1.19 and 1.21. The Ce and Eu anomalies were calculated using the following equations: $Ce / Ce^* = Ce_N / (La_N \times Pr_N)^{0.5}$ and $Eu / Eu^* = Eu_N / (Sm_N \times Gd_N)^{0.5}$ where subscript N indicates a PAAS normalized value.[10]

TABLE I. Literature values of *d*-spacing (*d*/Å) and intensity (*I*/%) for todorokite, birnessite, buserite and vernadite used to identify the manganese phase in coated structures from the Jabuka Pit

Todorkite South Africa (38-475)[a]		Todorkite Japan (13-164)[a]		Todorkite Cuba (18-1411)[a]		Synthetic todorkite Bilinski *et al.*[8]		Sample JP-103		Sample JP-104		Bimessite (43-456)[a]		Bimessite (23-1046)[a]		Bimessite (23-1239)[a]		Buserite (32-1128)[a]		Vernardite (15-604)[a]	
d	*I*	*d*	*I*	*d*	*I*	*d*	*I*	*d*	*I*	*d*	*I*	*d*	*I*	*d*	*I*	*d*	*I*	*d*	*I*	*d*	*I*
–	–	–	–	–	–	–	–	–	–	–	–	–	–	–	–	–	–	10.1	100	–	–
9.555	100	9.68	100	9.65	100	9.54	100	9.62	100	9.64	100	–	–	–	–	–	–	–	–	–	–
7.061	5	7.15	2	7.05	40	7.15	50	7.13	7	7.13	10	7.144	100	7.09	100	7.21	100	–	–	6.81	30
6.554	9	–	–	–	–	–	–	–	–	–	–	–	–	–	–	–	–	6.79	10	–	–
–	–	–	–	–	–	–	–	–	–	–	–	–	–	5.60	10	–	–	–	–	–	–
–	–	–	–	–	–	–	–	–	–	–	–	–	–	–	–	–	–	5.01	70	–	–
4.860	17	–	–	–	–	–	–	–	–	–	–	–	–	–	–	–	–	–	–	4.92	20
4.773	24	4.80	80	4.82	70	4.79	80	4.85	70	4.84	70	–	–	–	–	–	–	–	–	–	–
4.462	7	4.45	5	4.48	70	–	–	–	–	–	–	–	–	–	–	–	–	–	–	–	–
4.410	10	–	–	–	–	–	–	–	–	–	–	–	–	–	–	–	–	–	–	–	–
4.220	10	–	–	–	–	–	–	–	–	–	–	–	–	–	–	–	–	–	–	–	–
4.170	11	–	–	–	–	–	–	–	–	–	–	–	–	–	–	–	–	–	–	–	–
3.540	2	–	–	–	–	–	–	–	–	–	–	3.572	27	3.56	80	3.61	80	–	–	–	–
3.283	2	–	–	–	–	–	–	–	–	–	–	–	–	–	–	–	–	3.34	50	–	–
3.254	2	3.22	15	3.20	10	–	–	–	–	–	–	–	–	–	–	–	–	–	–	–	–
3.181	3	–	–	–	–	–	–	–	–	–	–	–	–	–	–	–	–	–	–	–	–
3.173	1	–	–	–	–	–	–	–	–	–	–	–	–	–	–	–	–	–	–	–	–
3.081	7	–	–	3.07	40	–	–	–	–	–	–	–	–	–	–	–	–	–	–	3.11	60
3.003	8	–	–	–	–	–	–	–	–	–	–	–	–	–	–	–	–	–	–	–	–
2.958	2	–	–	–	–	–	–	–	–	–	–	–	–	–	–	–	–	–	–	–	–
2.777	7	–	–	–	–	–	–	–	–	–	–	–	–	–	–	–	–	–	–	–	–
2.752	7	–	–	2.75	10	–	–	–	–	–	–	–	–	2.74	10	–	–	2.72	10	–	–
2.727	2	–	–	–	–	–	–	–	–	–	–	–	–	–	–	–	–	2.68	10	–	–
2.634	1	–	–	–	–	–	–	–	–	–	–	–	–	–	–	–	–	–	–	–	–
2.609	2	–	–	–	–	–	–	–	–	–	–	–	–	–	–	–	–	–	–	–	–
2.595	3	–	–	–	–	–	–	–	–	–	–	–	–	–	–	–	–	–	–	–	–
2.581	3	–	–	–	–	–	–	–	–	–	–	2.519	14	2.58	10	–	–	–	–	–	–
–	–	–	–	–	–	–	–	–	–	–	–	–	–	2.56	10	–	–	2.56	30	–	–
–	–	–	–	–	–	–	–	–	–	–	–	–	–	2.51	70	–	–	–	–	–	–
2.453	16	2.46	20	2.46	40	2.47	20	2.46	16	2.46	10	2.480	2	2.47	10	2.46	100	2.47	30	2.45	20
2.443	17	–	–	–	–	–	–	–	–	–	–	–	–	–	–	–	–	2.44	30	–	–
2.429	10	–	–	2.42	10	–	–	–	–	–	–	2.429	13	2.42	60	–	–	–	–	–	–
2.399	36	–	–	–	–	–	–	–	–	–	–	–	–	–	–	–	–	–	–	2.39	100
2.388	25	2.39	40	–	–	2.40	50	–	–	–	–	–	–	–	–	–	–	–	–	–	–
2.355	24	–	–	–	–	–	–	2.36	5	2.35	5	–	–	–	–	–	–	2.36	20	–	–
2.345	25	2.34	15	2.35	40	2.33	10	–	–	–	–	–	–	–	–	–	–	–	–	–	–
2.320	4	–	–	–	–	–	–	–	–	–	–	2.324	2	2.31	10	2.33	100	–	–	–	–
2.280	5	–	–	2.28	10	–	–	–	–	–	–	–	–	2.26	10	–	–	2.27	30	–	–
–	–	–	–	–	–	–	–	–	–	–	–	–	–	2.25	10	–	–	–	–	–	–
2.217	7	2.22	20	–	–	2.21	10	–	–	–	–	2.222	5	2.21	40	–	–	–	–	–	–
2.206	5	–	–	2.20	5	–	–	–	–	–	–	–	–	–	–	–	–	–	–	–	–
2.194	2	–	–	–	–	–	–	–	–	–	–	–	–	–	–	–	–	–	–	2.19	20
2.151	2	2.15	5	–	–	–	–	–	–	–	–	2.154	7	2.15	40	–	–	2.15	10	2.15	60
2.120	2	–	–	2.13	10	–	–	2.13	5	–	–	–	–	2.14	40	–	–	–	–	–	–
2.106	3	–	–	–	–	–	–	–	–	–	–	–	–	–	–	–	–	–	–	–	–
2.090	3	–	–	–	–	–	–	–	–	–	–	–	–	2.09	10	2.04	80	2.06	10	–	–
1.993	5	–	–	–	–	–	–	–	–	–	–	–	–	–	–	–	–	2.02	10	–	–
1.986	6	1.98	20	1.98	10	1.97	10	1.98	5	–	–	–	–	1.97	10	–	–	–	–	–	–
–	–	–	–	–	–	–	–	–	–	–	–	–	–	1.94	10	–	–	–	–	–	–
–	–	–	–	–	–	–	–	–	–	–	–	–	–	1.86	40	–	–	–	–	–	–
–	–	1.92	5	1.91	5	–	–	–	–	–	–	1.823	4	1.82	40	–	–	1.83	10	1.827	40
–	–	–	–	–	–	–	–	–	–	–	–	–	–	1.81	40	1.802	10	–	–	–	–
1.765	5	–	–	1.77	10	–	–	–	–	–	–	–	–	1.77	20	–	–	–	–	–	–
1.755	5	1.75	10	–	–	–	–	–	–	–	–	–	–	1.75	10	–	–	–	–	–	–
1.742	8	–	–	–	–	1.74	10	–	–	–	–	–	–	–	–	–	–	–	–	–	–
1.738	6	–	–	–	–	–	–	–	–	–	–	–	–	–	–	1.723	80	1.69	5	–	–
–	–	–	–	–	–	–	–	–	–	–	–	–	–	1.66	20	–	–	1.68	5	–	–
–	–	–	–	–	–	–	–	–	–	–	–	–	–	1.63	20	–	–	1.62	5	1.649	30
1.550	4	1.54	5	1.54	10	–	–	–	–	–	–	–	–	–	–	–	–	–	–	1.537	40
–	–	–	–	–	–	–	–	–	–	–	–	–	–	–	–	1.454	20	1.46	50	–	–
1.423	16	1.42	30	1.42	5	–	–	1.42	10	1.42	10	1.425	3	–	–	1.422	60	–	–	1.422	40
1.408	9	1.39	10	1.406	5	–	–	–	–	–	–	–	–	–	–	–	–	–	–	–	–

[a] Numbers in parantheses indicate JCPDF card number.

TABLE II. Chemical composition (mass fractions, *w*/%) of ferromanganese stalactitic aggregate (points T1–T13) and crust (points T15 and T16) as determined by EDS point count analyses[a],[b]

Sample point	Si	Al	Fe	Mn	Ti	Ca	Mg	Na	K	P	S	Ba	Ni	Co	V	Cl	O	Total	Mn/Fe	Mg/Mn
T1	0.7	1.6	n.d.	58.6	n.d.	1.5	6.7	2.0	0.5	0.1	0.5	0.4	0.5	0.1	n.d.	0.7	26.2	100	-	0.11
T2	5.1	2.8	3.6	46.0	n.d.	3.6	4.9	0.8	1.0	0.1	0.5	0.6	0.4	0.3	n.d.	0.7	29.6	100	12.6	0.11
T3	1.6	1.2	1.4	57.1	n.d.	2.8	6.8	0.8	0.5	n.d.	0.3	n.d.	0.3	n.d.	n.d.	0.7	26.6	100	40.1	0.12
T4	1.9	1.6	1.4	59.3	n.d.	1.9	5.4	0.3	0.6	n.d.	0.2	n.d.	0.3	n.d.	n.d.	0.7	26.4	100	43.9	0.09
T5	1.5	1.5	n.d.	60.4	n.d.	2.1	4.7	1.6	0.7	n.d.	0.3	n.d.	0.4	0.2	0.1	0.8	25.8	100	-	0.08
T6	1.1	1.6	n.d.	58.5	n.d.	2.2	7.0	2.4	0.4	n.d.	0.1	n.d.	n.d.	n.d.	n.d.	0.7	26.2	100	-	0.12
T7	2.1	2.6	n.d.	55.2	n.d.	1.5	7.4	2.0	0.5	n.d.	0.2	n.d.	0.3	n.d.	n.d.	0.9	27.3	100	-	0.13
T8	2.3	1.6	n.d.	38.4	n.d.	22.3[c]	4.3	1.1	0.8	n.d.	0.4	n.d.	0.3	n.d.	n.d.	0.4	28.2	100	-	0.11
T9	4.2	2.8	2.6	49.8	n.d.	1.9	6.0	0.7	0.1	n.d.	0.4	0.3	0.4	0.3	n.d.	0.8	30.0	100	19.1	0.12
T10	2.4	1.4	1.8	58.1	n.d.	1.2	4.7	1.8	0.9	n.d.	0.1	0.3	0.1	0.2	n.d.	0.6	26.4	100	32.1	0.08
T11	5.6	3.4	2.9	44.8	n.d.	2.6	6.3	1.2	1.2	n.d.	0.2	0.3	0.3	0.3	n.d.	0.9	30.0	100	15.2	0.14
T12	5.7	3.2	2.0	43.2	n.d.	5.7	5.1	0.6	1.4	n.d.	0.4	0.9	0.6	0.4	n.d.	1.2	29.8	100	21.5	0.12
T13	1.7	2.0	0.8	54.8	n.d.	2.1	6.3	1.2	1.0	n.d.	0.4	0.7	0.5	0.4	n.d.	1.6	26.5	100	66.0	0.11
T15	3.0	5.0	3.0	48.1	0.4	1.7	7.4	n.d.	0.6	0.1	0.1	n.d.	0.7	n.d.	n.d.	0.4	29.6	100	16.2	0.15
T16	3.6	3.9	1.9	48.2	n.d.	4.3	6.5	n.d.	0.8	n.d.	0.2	0.6	0.5	n.d.	n.d.	0.5	29.1	100	25.8	0.13

[a] The analyses correspond to ponits T1 to T16 plotted in Figure 3.
[b] n.d. – not detected.
[c] Detritad carbonate influence.

TABLE III. Chemical composition (mass fractions, *w*) of composite samples of ferromanganese stalactitic aggregates and crusts from various mollusk shells[a],[b]

	w / %													
Sample	SIO_2	Al_2O_3	Fe_2O_3	MnO	MgO	CaO	Na_2O	K_2O	TIO_2	P_2O_5	LOI/%	TOTAL/%		
JP-103	10.7	4.4	1.9	22.0	5.0	19.4	3.1	0.9	0.2	0.1	31.4	98.9		
JP-104	12.7	5.3	2.4	22.4	5.4	13.8	3.2	0.9	0.1	0.1	33.5	99.8		
V-13	n.d.	10.3	4.4	4.9	3.8	13.6	2.7	2.0	0.4	0.1	n.d.	n.d.		
	w / ppm													
Sample	Ba	Sr	Y	Zr	Be	V	Cu	Pb	Zn	Ni	Bi	Th	U	W
JP-103	1054	1013	10	36	1	172	123	74	109	1378	0.3	3.1	1.5	15.0
JP-104	960	1005	11	34	1	190	143	85	148	1293	0.3	3.5	1.6	18.0
V-13	213	495	20	44	2.2	105	32	14	95	140	n.d.	7.0	1.8	n.d.
	Tl	Ta	Hf	Cs	Au	As	Cr	Co	Rb	Nb	Mo	Sb		
JP-103	0.2	0.3	0.9	1.7	6	62	75	507	27	5.6	113	7.6		
JP-104	0.3	0.5	1.8	1.8	2	53	93	405	27	5.8	124	7.9		
V-13	n.d.	n.d.	n.d.	n.d.	n.d.	6	139	22	n.d.	n.d.	n.d.	n.d.		
	La	Ce	Pr	Nd	Sm	Eu	Gd	Tb	Dy	Ho	Er	Tm	Yb	Lu	Ce/Ce*
JP-103	11.1	32	2.325	9.77	2.07	0.49	1.76	0.33	1.85	0.37	1.11	0.168	0.98	0.154	1.45
JP-104	12	30.4	2.288	9.63	1.98	0.47	1.74	0.31	1.83	0.36	1.09	0.161	0.96	0.16	1.33
V-13	24	46.9	5.4	20.8	4.4	0.98	4.1	0.6	3.5	0.69	2	0.3	1.9	0.28	0.95

[a] Chemical composition of surficial sediment (sample V-13) is taken from Dolenec *et al.*[4]
[b] n.d., not determined.

DISCUSSION AND CONCLUSIONS

The heterogeneity, cryptocrystallinity or very fine particle size of the ferromanganese-coated structures from the Jabuka Pit made identification of their mineralogy by means of X-ray diffraction difficult and almost impossible. The occurrence of carbonates, silicates and clay minerals admixed with the ferromanganese minerals in coated structures caused an additional complication, because their X-ray lines can sometimes be confused with those of manganese oxides. However, the strongest peaks at 9.62 and 9.64 Å, as well as those at 4.84 and 4.85 Å, and the medium to weak reflections at 7.13 Å, 2.46 Å, 2.35 and 2.36 Å, 2.28 Å, 2.13Å, 1.98 Å and 1.42 Å suggest that the main constituents of the ferromanganese crusts and collomorph-banded as well as botryoidal aggregates are 10 Å manganese hydroxides. The investigated samples show values of *d*-spacing

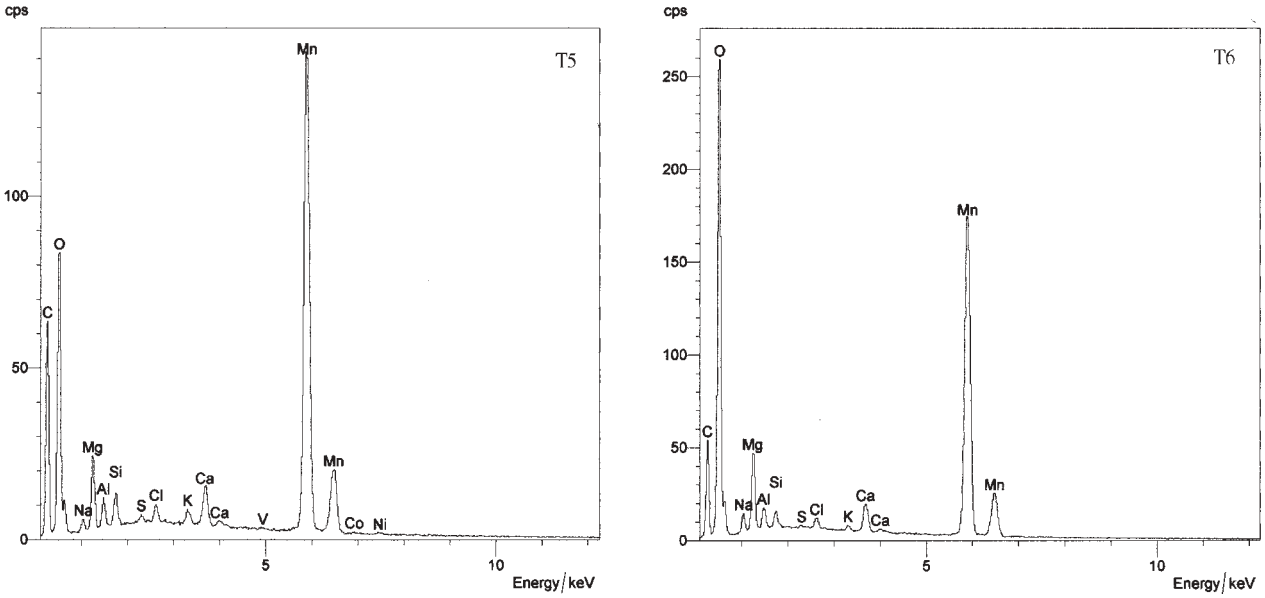

Figure 4. Energy Dispersive Spectroscopy (EDS) of the dark-grey (T5) and light-grey (T6) ferromanganese layer from Figure 3 showing differences in the height of the oxygen peak between the dark and bright layers.

similar to natural and synthetic todorokite but not to the patterns of buserite, birnessite or vernadite (Table I). However, we must point out that due to the relatively low crystallinity of the investigated ferromanganese coated structures and their admixture with other authigenic and detrital minerals we were unable to ascertain if the 7.13 Å reflection in both samples corresponds either to a 10 Å manganate mineral phase, or a 7 Å layer-structured phyllomanganate birnessite (Table I). A reflection at approximately 7 Å is usually attributed to birnessite.[11] Although in our set of XRD data relatively strong peaks of birnessite (*i.e.* those at 3.6 Å, 2.46 Å, 2.33 Å, 2.04 Å and 1.723 Å) are missing or masked by reflections of the 10 Å manganate phase, we were not able to exclude the possible presence of birnessite. Because the diffraction lines of 10 Å manganates also overlap the characteristic X-ray diffraction lines at 2.40–2.45 Å and 1.40–1.45 Å of vernadite[11] it is also impossible to determine the presence of this mineral in our samples. Thus, for more precise identification of the crystalline phases in the ferromanganese crusts and coatings from the Jabuka Pit further studies such as contraction and expansion tests, differential scanning calorimetry (DSC) and Mössbauer spectroscopy are necessary.

A significant feature of the predominantly 10 Å manganate coated structures from the Jabuka Pit is their considerable enrichment in Mg. Mandernack *et al.*,[12] have suggested that replacement of Mn^{II} by Mg stabilizes the 10 Å manganate structure. The Mg/Mn mass ratio of the 10 Å manganate samples analyzed in this study varies from 0.08 to 0.15 (Table I) and compares very well with Mg/Mn values in the range between 0.08 and 0.15 for 10 Å Mn^{IV} manganates of microbial origin.[12]

The predominantly 10 Å manganate coated structures from the Jabuka Pit are also an important trace-metal bearing mineral phase, showing higher concentrations of Ni, Ba and Co, as well as Cu, Pb and Zn, relative to the surficial sediment (Tables II and III). These elements are, according to Koschinsky and Halbach,[13] present in seawater mainly as hydrated and labile complexed cations. The abundance of a given element in the ferromanganese coated structures from the Jabuka Pit seems to be controlled primarily by scavenging processes during precipitation of Mn and Fe oxides but can also be influenced by other factors such as the amount of dissolved O_2 in the bottom seawater and the sources of the elements.

The exact mechanisms of formation of predominantly 10 Å manganate crusts and coatings in the Jabuka Pit are still unknown. The three accretionary modes of hydrogenous precipitation, oxic and suboxic diagenesis have been suggested for Mn precipitation in the marine environment.[14,15,16] Since coated structures were found in the Jabuka Pit only on surfaces exposed to seawater, we believe that they are essentially hydrogenetic.

The relatively high concentration of Ce and a strong positive Ce anomaly in the investigated samples (Figure 5) suggest a highly oxidizing environment during their formation. According to Nath *et al.*,[17] the high content of Ce and higher values of Ce anomalies in ferromanganese nodules and crusts of hydrogenous origin is to be attributed to a highly oxidizing environment. Buljan and Zore-Armanda also indicated oxidizing conditions in the Jabuka Pit.[18] Strong positive Ce anomalies have often been reported in manganese nodules and crusts from different localities.[19,20] However, in a few cases negative

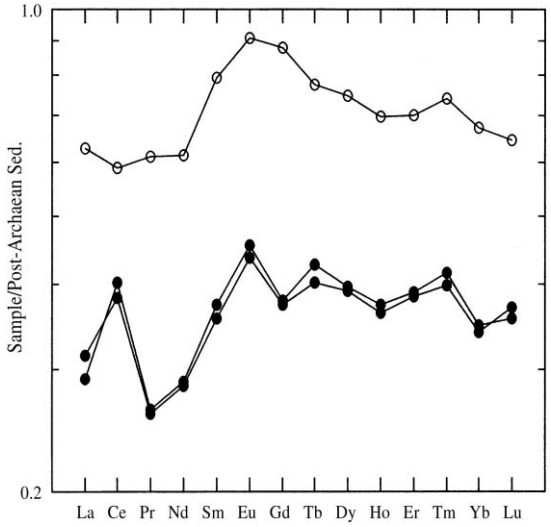

Figure 5. Post-Archean average Australian shale (PAAS) normalized REE patterns of ferromanganese composite samples JP-103 and JP-104 (●) and surficial sediment V-13 (○) from the Jabuka Pit.

Ce anomalies in ferromanganese nodules and crusts were also reported. [21,22]

The formation of predominantly 10 Å manganate crusts and stalactitic structures at the sediment-water interface is obviously caused by a supply of Mn and other trace metals from the near-bottom seawater. The Mn content of bottom seawater appears to be mainly controlled by redistribution of Mn in surficial sediment due to oxic diagenesis. The release of Mn from surface sediment in the Jabuka Pit during oxic diagenesis is supported by the Mn enrichment found within the upper 0–5 cm of the sediment and its decrease in the deeper parts, as noted by Paul and Meishner[23] and Kosta *et al*.[5] The topmost part (0–5 cm) of the surficial sediment from the Jabuka Pit contains up to 4250 ppm of Mn, while the Mn concentrations in sediments from deeper sections (5–15 cm) are considerably lower (up to 1300 ppm). In contrast, only slightly lower Fe concentrations within the upper 0–5 cm of the sediment (3.6 %) as compared to the values (3.9 %) in deeper sediments indicate that Fe remains more or less bound in the sediment.[5]

Acknowledgement. – This research was performed with financial support from the Ministry of Science and Technology, Republic of Slovenia (Project MZT J1-07331 and Bilateral Project between Croatia and Slovenia 1997–1999) and Geoexp, d. o. o., Tržič. Slovenia. To both of these institutions I express my sincere thanks. I also thank the reviewers, whose constructive comments contributed significantly to improving the manuscript. Thanks also go to lector Anthony Byrne for correcting the English.

REFERENCES

1. J. Faganeli, J. Pezdič, B. Ogorelec, M. Mišič, and M. Najdek, *Continental Shelf Research* **14** (1994) 365–384.
2. L. M. J. U. Van Straaten, *Geol. Rundsch.* **60** (1970) 106–131.
3. A. Damiani, *Boll. Soc. Adriat. Sci*. **53** (1965) 197–210.
4. T. Dolenec, J. Faganeli, and S. Pirc, *Geol. Croat.* **51** (1998) 59–73.
5. L. Kosta, V. Ravnik, A. R. Byrne, J. Štirn, M. Dermelj, and P. Stegnar, *J. Radioanal. Chem*. **44** (1978) 317–332.
6. T. Dolenec, *RMZ – Material and Geoenvironment,* **46** (1999) 443–447.
7. R. G. Burns and V. M. Burns, *Nature* **155** (1975) 130–131.
8. H. Bilinski, R. Giovanoli, A. Usui, and D. Hanžel, *Am. Mineral*. **87** (2002) 580–591.
9. G. Lei and K. Boström, *Mar. Geol.* **123** (1995) 253–261.
10. S. R. Taylor and S. M. McLennan, *The Continental Crust: Its Composition and Evolution*. Blackwell, Oxford, 1985, p. 312.
11. R. G. Burns and V. M. Burns, *Min. Soc. Am. Short Course Notes* **6** (1979) 1–46.
12. K. W. Mandernack, J. Post, and M. T. Bradley, *Geochim. Cosmochim. Acta* **59** (1995) 4393–4408.
13. A. Koschinsky and P. Halbach, *Geochim. Cosmochim. Acta* **24** (1995) 5113–5132.
14. P. N. Froelich, G. Klinkhammer, M. Bender, N. A. Luedki, G. R. Heath, D. Cullen, P. Dauphin, D. Hammond, B. P. Hartman, and V. Maynard, *Geochim. Cosmochim. Acta* **43** (1979) 1075–1090.
15. S. Emerson, R. Jahnke, M. Bender, P. N. Froelich, G. Klinkhammer, C. Bowser, and G. Setlock, *Earth Planet. Sci. Lett.* **49** (1980) 57–80.
16. J. N. Pattan, *Mar. Geol*. **97** (1993) 331–344.
17. B. N. Nath, J. Roelandts, M. Sudhakar, W. L. Plüger, and V. Balaram, *Oceanogr. Mar. Geol*. **120** (1994) 385–400.
18. M. Buljan and M. Zore-Armanda, *Acta Adriat*. **20** (1979) 1–368.
19. B. N. Nath, V. Balaram, M. Sudhakar, and A. Plüger, *Mar. Chem*. **38** (1992) 185–208.
20. A. J. Fleet, *Aqueous and sedimentary geochemistry of the rare earth*, in: P. Henderson (Ed.), *Rare Earth Element Geochemistry*, Elsevier, Amsterdam, 1984, pp. 343–373.
21. J. W. Moffet, *Geochim. Cosmochim. Acta* **58** (1994) 695–703.
22. X. Wen and E. H. De Carlo, *EDS Trans. Geophys. Union* **74** (1994) 78.
23. J. Paul and D. Meishner, *Shenckenbergiana Marit.* **8** (1976) 91–102.

SAŽETAK

Nataložene feromanganske strukture iz Jabučke Kotline (Središnji Jadran): mineraloška, geokemijska i genetska razmatranja

Tadej Dolenec

Jedna od najinteresantnijih osobina Jabučke Kotline, depresije do 275 m u Središnjem Jadranu, je prisustvo feromanganskih prevlaka nađenih na različitim ljušturama mekušaca, fragmentima ljuštura i na drugom biogenom detritusu u kontaktu s morskom vodom. Te su prevlake sastavljene uglavnom od Fe-siromašnih i Mg-bogatih 10 Å manganata. 10 Å manganati također čine kolomorfne forme i grozdaste agregate, a također 1,5 mm stalaktitne strukture sastavljene od pločastih kristala duljine do 5 μm. Pretpostavlja se hidrogeno taloženje na granici faza sediment/voda u oksidativnim uvjetima.